Non-cooperative Games to Control Learned Inverter Dynamics of Distributed Energy Resources

Paul Serna-Torre[a,b], Vishal Shenoy[c], David Schoenwald[d], Jorge I. Poveda[c], and Patricia Hidalgo-Gonzalez[a,b,c]

[a] Department of Mechanical and Aerospace Engineering, University of California, San Diego, CA 92093, United States
[b] Center for Energy Research, University of California, San Diego, CA 92093, United States
[c] Department of Electrical and Computer Engineering, University of California, San Diego, CA 92093, United States
[d]Sandia National Laboratories, Albuquerque, NM 87185, USA
{psernatorre, vshenoy, poveda, phidalgogonzalez}@ucsd.edu, daschoe@sandia.gov

Abstract—We propose a control scheme via a non-cooperative linear quadratic differential game to coordinate the inverter dynamics of Distributed Energy Resources (DERs) in a microgrid (MG). The MG can provide regulation services in support to the upper-level grid, in addition to serving its own load. The control scheme is designed for the MG to track a power reference, while each DER seeks to minimize its individual cost function subject to *learned inverter dynamics* and load perturbations. We use a nonlinear high-fidelity model developed by Sandia National Laboratories to learn inverter dynamics. We determine a Nash strategy for the DERs that uses state estimation of a Loop Transfer Recovery. Results show that the control scheme enables savings up to 9.3 to 208 times in the DERs objective cost functions and a time-domain response with no oscillations with up to 3 times faster settling times relative to using droop and PI control.

Index Terms—Ancillary services, control of voltage-source inverters, learned inverter dynamics, non-cooperative differential game, smart grid.

I. INTRODUCTION

Distributed Energy Resources (DERs) can be harnessed to tackle local operational issues such as voltage and frequency fluctuations in a microgrid (MG) or in a distribution grid [1], [2]. In addition to addressing local issues, they can also assist the upper-level grid, e.g. the transmission grid, in solving operational challenges.

Although DERs are geographically dispersed and belong to different owners, they can be coordinated to work as a Virtual Power Plant (VPP) [3] to provide regulation services in support to the upper-level grid operation [4], [5], [6]. Indeed, governments are increasingly fostering the integration of DERs in microgrids into ancillary service markets for the provision of regulation services to the transmission grid at the system operator's request [7].

A body of work on the control of DERs for the provision of regulation services has been proposed from the optimization perspective. For instance, the work in [8] proposes an online algorithm that drives DERs' power outputs so that the net power delivered from the distribution grid to the transmission grid tracks a power reference. This online algorithm is based on an AC Optimal Power Flow formulation using primal-dual-gradient methods in which the distribution grid pursues the optimal trajectory while satisfying the power reference tracking. In [9], the authors develop a bidding strategy for a VPP in which the customer load is satisfied and simultaneously the VPP is able to sell load-following ancillary services to Western Australian grid. The work in [10] proposes a linear programming model to maximize the profit of a DER aggregator by controlling the charge of electric vehicles (EVs) and by providing day-ahead reserve services to the transmission grid or other stakeholders. For further references on this topic the reader may refer to [11], [12], [13].

While optimization-based methods hold promise for online implementation and fast computation, these approaches rely on optimizing global economic satisfaction for both the operator and DERs. This approach can disregard the fact that DERs belong to different owners who may be selfish and seek to optimize their individual economic interests. One way to address this limitation is by using non-cooperative game theory to coordinate DERs to provide regulation services. In fact, the extensive survey in [14] remarks that non-cooperative games, among other game-theoretic approaches, is the most widely used coordination method (in academia) for demand response and DERs in electricity markets. The works in [15], [16] propose game theoretic-based frameworks to coordinate the charging/discharging power of EVs such that the EVs' aggregators can trade that amount of energy with the upper-level grid to support frequency regulation. For a more complete literature review on the coordination of DERs to provide ancillary services using Game Theory, we refer the reader to [17], [18]. Moreover, for local regulation services, the work in [19] develops a Nash equilibrium-based control scheme to coordinate DERs in an islanded MG to bring frequency deviations back to zero. The authors of [20] propose a non-cooperative differential game control scheme to steer the state

of a MG to nominal operating conditions by controlling the input impedance of storage units.

However, to the best of our knowledge, non-cooperative game-based work for control of DERs does not: (i) consider nonlinear high-fidelity dynamics of the voltage-source inverter (VSI) with its associated control loops, or (ii) implements the resulting controllers in a grid with VSIs.

The increasing deployment of DERs opens the question on how to coordinate DERs for the provision of regulation services to the upper-level grid considering nonlinear high-fidelity dynamics of VSIs. To the best of our knowledge, there is no previous work addressing this challenge from a non-cooperative game theory perspective.

II. Contributions

The contributions of this work are:

- To propose, for the first time, a non-cooperative game framework that incorporates learned VSI dynamics of DERs from a nonlinear high-fidelity model to represent their participation in a VPP to meet regulation services in support to the upper-level grid. We illustrate this framework in the context of regulating real power injections.
- To show the cost effectiveness and time-domain performance of our proposed control scheme compared with classic control techniques such as droop control and proportional-integral (PI) control.
- To provide guidelines to the system operators to develop and implement non-cooperative differential games that incorporate VSI dynamics.

III. Problem Formulation

A. Overview

We consider a MG that consists of photovoltaic (PV) panels, Battery Electricity Storage Systems (BESS), loads, and a connection with the upper-level grid. The control scheme we propose consists of a controller for each DER to steer the VSI using *dq*-frame control loop dynamics. This control scheme enables the MG to provide a regulation service for the upper-level grid. This regulation service consists of a power reference that the MG's power output must track. We use the term *upper-level grid* because a MG can supply power to the distribution or transmission network.

First, we formulate a state-space representation of the MG that groups the learned VSI dynamics of DERs and a compensator. The compensator models the tracking error dynamics of the MG's power output relative to the power reference. We use system identification (SI) to learn transfer functions from a high-fidelity model of each DER considering its VSI dynamics using a *dq*-frame control loop.

Second, we design a control scheme for DERs via a non-cooperative linear quadratic differential game. Under this approach, each DER seeks to minimize its individual linear quadratic cost subject to the MG's state-space representation.

Third, we find the Nash equilibrium of the non-cooperative game, and then, we determine the state feedback control for each DER. Since all the states of each DER are not accessible,

we use Loop Transfer Recovery for each DER that estimates all DER's state. We feed the DERs' estimated states and the dynamic compensator's states into the controller of each DER.

Fourth, we validate the control scheme by checking parity in cost solutions and simulation performance of: (i) the MG's state-space representation that has learned DERs dynamics, and the three-phase MG with high-fidelity DERs dynamics. Each high-fidelity DER model has a VSI and uses a *dq*-frame control loop, which was designed in [21], [22], [23] by Sandia National Laboratories.

Lastly, we compare the cost effectiveness and time-domain performance of the control scheme we propose against the classical droop control and PI control across a set of MGs with different numbers of DERs.

B. Assumptions

In this work, we assume that the MG connects with the upper-level grid which imposes frequency and voltage at nominal values at the point of connection. The DERs engaged in the provision of regulation service communicate complete information about their states to each other. The matrix pair (A_i, B_i) of the state-space realization of each DER is controllable, which is a design choice.

C. Control Scheme Design

1) Learned voltage source inverter (VSI) dynamics: In this work, we assume a PV panel or BESS that uses a *dq*-frame control loop for its VSI that regulates the DER's active/reactive power output according to a reference input [24].

We use SI to represent the dynamics of the VSI and its *dq* control loop into one dynamical system for each DER. SI is a method that identifies the transfer function of a dynamical system from observed input-output data [25]. We use the SI approach under a non-linear least squares with automatic line search method to learn the dynamics of each DER instead of deriving its full white-box model because: (i) DERs' owners may not disclose the full model of their DER due to privacy concerns, and (ii) each DER may contain multiple control loops resulting in a state-space representation with high computational complexity.

2) Virtual power plant and compensator: A learned time-invariant state-space representation models the VSI-based DER dynamics. In this learned model generated by SI, the state $x_i(t) \in \mathbb{R}^d$ does not necessarily represent physical quantities. The i-th DER can regulate its active power output $y_i(t) \in \mathbb{R}$ by regulating the control input $u_i(t) \in \mathbb{R}$. From here onwards we will drop the explicit dependence with time t when it can be inferred from the context, e.g., in our notation $x_i(t)$ is equivalent to x_i. The dynamics of each DER are expressed as follows

$$\dot{x}_i = A_i x_i + B_i u_i \tag{1}$$

$$y_i = C_i x_i, \tag{2}$$

where $A_i \in \mathbb{R}^{d \times d}$, $B_i \in \mathbb{R}^{d \times 1}$, $C_i \in \mathbb{R}^{1 \times d}$. The DERs are connected in parallel to a single bus in the MG. Fig. 1 illustrates a MG with two DERs and a load. In this way, the

state-space representation of the VPP (augmented dynamics) that groups the DERs can be expressed as

$$\begin{bmatrix} \dot{x}_1 \\ \vdots \\ \dot{x}_N \end{bmatrix} = \begin{bmatrix} A_1 & & \\ & \ddots & \\ & & A_N \end{bmatrix} \begin{bmatrix} x_1 \\ \vdots \\ x_N \end{bmatrix} + \begin{bmatrix} B_1 & & \\ & \ddots & \\ & & B_N \end{bmatrix} \begin{bmatrix} u_1 \\ \vdots \\ u_N \end{bmatrix} \tag{3}$$

$$y = \begin{bmatrix} C_1 & \dots & C_N \end{bmatrix} \begin{bmatrix} x_1 \\ \vdots \\ x_N \end{bmatrix}, \tag{4}$$

where N is the number of DERs in the MG. In a more compact
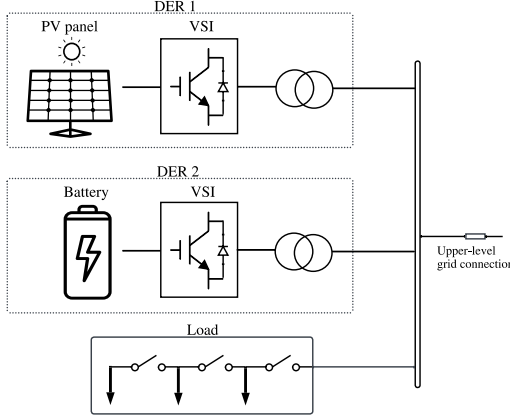

Fig. 1. Microgrid (MG) with two VSI-interfaced DERs: one PV system and one BESS. The MG has a load and a connection with the upper-level grid.

form, the state-space representation of the VPP is denoted by

$$\dot{x} = Ax + Bu \tag{5}$$

$$y = Cx, \tag{6}$$

where $x = \begin{bmatrix} x_1 & \dots & x_N \end{bmatrix}^\top \in \mathbb{R}^{N \cdot d}$, A, B and C are the corresponding block matrices from (3) and (4). In (6), $y(t)$ is the active power output of the VPP. Since a load, $d(t) \in \mathbb{R}$, is connected to the MG, the net power delivered to the upper-level grid is $y(t) - d(t)$.

We represent the power reference of the regulation service by $p_{\text{req}}(t) \in \mathbb{R}$. In this regulation service, the MG's power delivered to the upper grid $y(t) - d(t)$ must track the requested power $p_{\text{req}}(t)$. Equivalently, the VPP's power generation $y(t)$ must track the reference $r(t) = p_{\text{req}}(t) + d(t)$.

In order for the MG to comply with the power regulation service, we propose a compensator of the form

$$\dot{w} = Hw + Ge \tag{7}$$

$$v = Dw, \tag{8}$$

where $w(t)$, $v(t) \in \mathbb{R}$, and $e(t)$ represents the tracking error of $y(t)$ with respect to $r(t)$ defined as follows

$$e(t) := r(t) - y(t) = r(t) - Cx(t). \tag{9}$$

The matrices H, G, and $D \in \mathbb{R}$ are chosen according to the desired structure of the compensator. Using (5)-(9),

the augmented state-space representation that includes the dynamics of the VPP and compensator can be written as

$$\begin{bmatrix} \dot{x} \\ \dot{w} \end{bmatrix} = \begin{bmatrix} A & 0 \\ -GC & H \end{bmatrix} \begin{bmatrix} x \\ w \end{bmatrix} + \begin{bmatrix} \bar{B}_1 & \dots & \bar{B}_N \end{bmatrix} u + \begin{bmatrix} 0 \\ G \end{bmatrix} r \tag{10}$$

$$\begin{bmatrix} y \\ v \end{bmatrix} = \begin{bmatrix} C & 0 \\ 0 & D \end{bmatrix} \begin{bmatrix} x \\ w \end{bmatrix}, \tag{11}$$

where $\bar{B}_i = \begin{bmatrix} 0 & \dots & B_i & \dots & 0 \end{bmatrix}^\top$.

3) Deviation form of the augmented system: We introduce auxiliary states for the DERs and the compensator defined as

$$\widetilde{x}(t) = x(t) - x_{\text{ss}} \tag{12}$$

$$\widetilde{w}(t) = w(t) - w_{\text{ss}}, \tag{13}$$

where x_{ss} and w_{ss} are the states achieved when the tracking error $e(t)$ becomes zero. In the same manner, we express $\widetilde{e}(t)$ as follows

$$\widetilde{e}(t) = e(t) - e_{\text{ss}} = r(t) - Cx(t) - (r(t) - Cx_{\text{ss}}) = -C\widetilde{x}(t). \tag{14}$$

Using (12) - (14) and similarly defining $\widetilde{u}(t)$, $\widetilde{y}(t)$ and $\widetilde{v}(t)$, we construct the state-space representation of the augmented system in deviation form as follows

$$\begin{bmatrix} \dot{\widetilde{x}} \\ \dot{\widetilde{w}} \end{bmatrix} = \bar{A} \begin{bmatrix} \widetilde{x} \\ \widetilde{w} \end{bmatrix} + \begin{bmatrix} \bar{B}_1 & \dots & \bar{B}_N \end{bmatrix} \widetilde{u} \tag{15}$$

$$\begin{bmatrix} \widetilde{y} \\ \widetilde{v} \end{bmatrix} = \bar{C} \begin{bmatrix} \widetilde{x} \\ \widetilde{w} \end{bmatrix}, \tag{16}$$

where $\bar{A} = \begin{bmatrix} A & 0 \\ -GC & H \end{bmatrix}$, $\bar{B}_i = \begin{bmatrix} 0 & \dots & B_i & \dots & 0 \end{bmatrix}^\top$, and $\bar{C} = \begin{bmatrix} C & 0 \\ 0 & D \end{bmatrix}$.

We also note that when the original augmented system (10) - (11) begins to track an input reference $r(t)$, its corresponding deviation system (15) - (16) is out of the equilibrium since $x(t_0) - x_{\text{ss}} \neq 0$ and $w(t_0) - w_{\text{ss}} \neq 0$. Finally, when the tracking error is zero at t_*, then $\widetilde{x}(t_*) = x(t_*) - x_{\text{ss}} = 0$ and $\widetilde{w}(t_*) = w(t_*) - w_{\text{ss}} = 0$ which indicates that the deviation system is at the origin. Therefore, a tracker problem for the augmented system is actually equivalent to a regulator problem for its corresponding deviation system [26].

4) Non-cooperative linear quadratic differential game for DER coordination: We consider DERs that belong to different owners, i.e., *players*, such that each DER seeks to minimize its individual linear quadratic cost $J_i(\widetilde{x}_0, \widetilde{w}_0, \widetilde{u})$ during the power regulation service. This cost is given by

$$J_i(\widetilde{x}_0, \widetilde{w}_0, \widetilde{u}) = \int_{t_0}^\infty \left\{ \begin{bmatrix} \widetilde{x} \\ \widetilde{w} \end{bmatrix}^\top Q_i \begin{bmatrix} \widetilde{x} \\ \widetilde{w} \end{bmatrix} + \widetilde{u}_i^\top R_i \widetilde{u}_i \right\} dt, \tag{17}$$

where $\widetilde{x}_0$ is the DER's deviation state vector (12) at t_0, $\widetilde{w}_0$ is the compensator's deviation state (13) at t_0, and $\widetilde{u}$ is the strategy that steers $[\widetilde{x} \ \widetilde{w}]^\top$ to the origin.

We highlight that the individual cost of the i-th DER (17) is affected not only by its own strategy $\widetilde{u}_i$, but it is also implicitly affected by the strategies of the other DERs that participate in
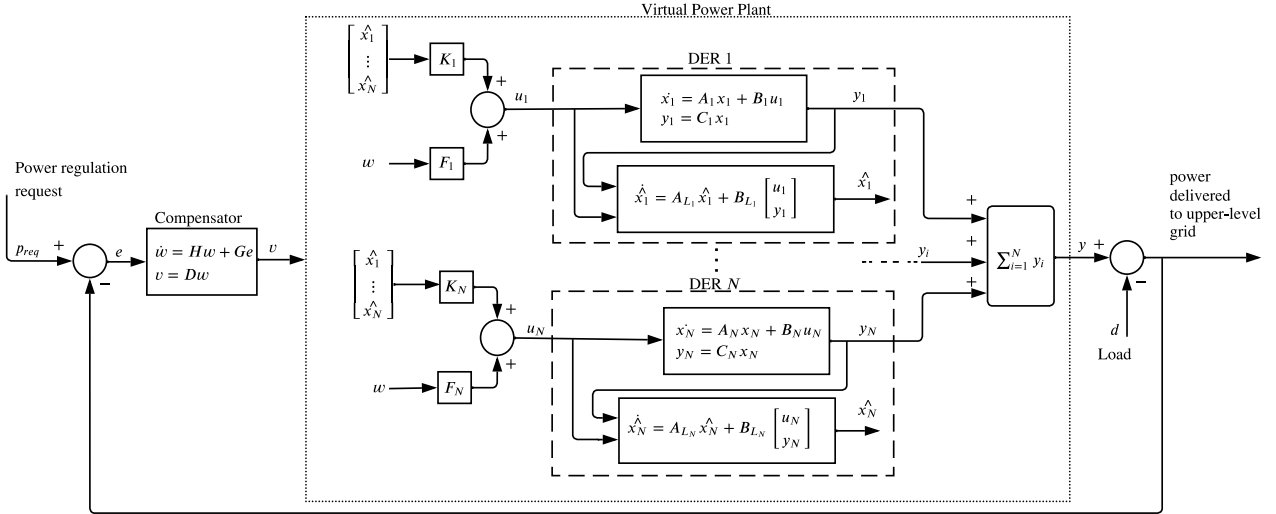
Fig. 2. Control scheme for a microgrid (MG) to provide power regulation service in support to the upper-level grid. Although N DERs seek to minimize their individual cost objective, they work as a virtual power plant such that the MG's power delivered to the grid complies with the power regulation request. For each DER i, a state-space representation $[A_i, B_i, C_i]$ models the VSI and dq-control loop dynamics, and a Loop Transfer Recovery $[A_{Li}, B_{Li}, C_{Li}]$ estimates the state $\hat{x}_i$. A compensator $[H, G, D]$ models the tracking error dynamics of the MG's power output with respect to the requested power. Each DER i employs a state-feedback Nash control $[K_i, F_i]$ that is fed by estimated states $[\hat{x}_1, ..., \hat{x}_N]^\top$ and the compensator's state w.

the regulation service because it considers all the states. The matrices $Q_i = Q_i^\top \geq 0$ and $R_i \geq 0$ are the state weighting matrix and the control weighted matrix, respectively.

We can reformulate the individual cost of the i-th DER (17) to make it easy to interpret by expressing Q_i as follows:

$$Q_i = \begin{bmatrix} q_{i,1}C_1^\top C_1 & & & \\ & \ddots & & \\ & & q_{i,N}C_N^\top C_N & \\ & & & q_{i,w} \end{bmatrix}, \quad (18)$$

where C_i is the output matrix of the state-space representation of the i-th DER (2), and $q_{i,1}, ..., q_{i,N} \in \mathbb{R}$ are factors chosen by the i-th DER. Using (18) and (17) we obtain

$$J_i(\widetilde{x}_0, \widetilde{w}_0, \widetilde{u}) = \int_{t_0}^\infty \{ \sum_{j=1}^N q_j \widetilde{y}_j^2 + p_w \widetilde{w}^2 + \widetilde{u}_i^\top R_i \widetilde{u}_i \} \, dt. \quad (19)$$

Each DER i adjust its factors $\{q_{i,1}, ...q_{i,N}\}$ according to its incentive to penalize the departure of the power output vector y away from the vector y_{ss}. The factor $q_{i,w}$ reflects the incentive of the DER to take a high share of power in the provision of the regulation service. If the DER i sets $q_{i,w}$ to a high value, its power share in the power regulation service may be less than other DERs that set the factor to lower values.

On the other hand, R_i reflects the cost that the i-th DER assigns to its available energy for the power regulation service. A high value of R_i means that the DER i regards its energy source, e.g., solar energy, as expensive for the power regulation service.

The non-cooperative game consists of the minimization of the individual linear quadratic cost (17) for $i = \{1, ..., N\}$,

subject to the dynamical system described in (15) - (16). Each DER employs a linear feedback strategy given by

$$\widetilde{u}_i = \begin{bmatrix} K_i & F_i \end{bmatrix} \begin{bmatrix} \widetilde{x} \\ \widetilde{w} \end{bmatrix}, \quad (20)$$

where $K_i \in \mathbb{R}^{1 \times N \cdot d}$, and $F_i \in \mathbb{R}$. Using (12) and (13), we can express the control strategy as a function of the states $x(t)$ and $w(t)$ as follows

$$u_i - u_{ss} = \begin{bmatrix} K_i & F_i \end{bmatrix} \begin{bmatrix} x - x_{ss} \\ w - w_{ss} \end{bmatrix} \quad (21)$$

$$u_i = \begin{bmatrix} K_i & F_i \end{bmatrix} \begin{bmatrix} x \\ w \end{bmatrix}. \quad (22)$$

The set of feedback strategies $\{u_1, \ldots, u_N\}$ is admissible if the eigenvalues of the closed-loop system are in the left half-plane. A necessary and sufficient condition for this set to not be empty is that $(\bar{A}, \begin{bmatrix} \bar{B}_1 & ... & \bar{B}_N \end{bmatrix})$ is stabilizable [27], [28].

We determine the set of admissible strategies $\{u_1, \ldots, u_N\}$ of the form (22) using the concept of Nash equilibrium [29], which requires the equilibrium strategies $\widetilde{u}_i^*$ to satisfy the following inequality

$$J_i(\widetilde{x}_0, \widetilde{w}_0, \widetilde{u}^*) \leq J_i(\widetilde{x}_0, \widetilde{w}_0, \widetilde{u}_{-i}^*), \quad (23)$$

for $i = \{1, 2, ..., N\}$, where $\widetilde{u}^* = \begin{bmatrix} \widetilde{u}_1^* & ... & \widetilde{u}_N^* \end{bmatrix}^\top$, and $\widetilde{u}_{-i}^* = \begin{bmatrix} \widetilde{u}_1^* & ... & \widetilde{u}_{i-1}^* & \widetilde{u}_i & \widetilde{u}_{i+1}^* & ... & \widetilde{u}_N^* \end{bmatrix}^\top$. Inequality (23) means no DER can improve its optimal individual cost, $J_i(\widetilde{x}_0, \widetilde{w}_0, \widetilde{u}^*)$, by a unilateral deviation from its equilibrium strategy $\widetilde{u}_i^*$. As [30] indicates, the Nash strategy for player i can be explicitly computed to be

$$u_i^* = -R_i^{-1} \bar{B}_i P_i \begin{bmatrix} x \\ w \end{bmatrix} \quad (24)$$

for $i = \{1, ..., N\}$, where the matrices P_i are the symmetric stabilizing solution of the coupled Algebraic Riccati equations:

$$\left(\bar{A} - \sum_{j \neq i}^{N} S_j P_j\right)^{\top} P_i + P_i \left(\bar{A} - \sum_{j \neq i}^{N} S_j P_j\right) - P_i S_i P_i + Q_i = 0 \tag{25}$$

for $i = \{1, ..., N\}$, where: $S_i = \bar{B}_i R_i^{-1} \bar{B}_i^{\top}$. Moreover, the optimal cost solution of DER i in the Nash equilibrium is given by

$$J_i(\widetilde{x}_0, \widetilde{w}_0, \widetilde{u}^*) = \begin{bmatrix} \widetilde{x}_0 \\ \widetilde{w}_0 \end{bmatrix}^{\top} P_i \begin{bmatrix} \widetilde{x}_0 \\ \widetilde{w}_0 \end{bmatrix}. \tag{26}$$

We remark that the Nash strategy (24)) steers the deviation state $[\widetilde{x} \quad \widetilde{w}]^{\top}$ to the origin. Due to the equivalence of the regulator problem and the tracker problem that we explain in Section III-C3, the Nash strategy (24)) also results in $y(t)$ tracking the reference input $r(t)$. Hence, the MG complies with the power regulation service when the DERs employ the Nash strategy (24)).

There have been extensive efforts [27], [31], [32], [33], [34], [35] to solve the coupled Riccati equations (25). In this work, we employ an iterative algorithm based on the reference [35]. We finds stabilizing solutions P_i^k of the iteration k of the N non-coupled Riccati equations

$$(A_i^{k-1})^{\top} P_i^k + P_i^k A_i^{k-1} - P_i^k S_i P_i^k + Q_i = 0 \tag{27}$$

for $i = \{1, ..., N\}$. The matrices $A_i^{k-1} := \bar{A} - \sum_{j \neq i}^{N} S_j P_j^{k-1}$ are calculated using the stabilizing solutions of a previous iteration. The algorithm stops when $\sigma(\bar{A} - \sum_{i=1}^{N} S_i P_i^k) \in \mathbb{C}^-$.

5) Loop Transfer Recovery (LTR) for DERs: Since the proposed controllers are state feedback controllers and the states of the DERs are inaccessible, we design a LTR for each DER to estimate the state x_i. The system parameters $[A_{Li} \; B_{Li} \; C_{Li}]$ of the LTR are the following

$$A_{Li} = A_i + \Delta A_i - L_i(C_i + \Delta C_i) \tag{28}$$

$$B_{Li} = [B_i + \Delta B_i \quad L_i] \tag{29}$$

$$C_{Li} = I_{dxd}, \tag{30}$$

where the gain L_i is a Kalman filter gain iteratively tuned so that the closed-loop DER system loop gain using L_i approaches the loop gain using full state feedback. In this manner, despite the parameter perturbations $\Delta A_i, \Delta B_i$, and ΔC_i, the LTR can recover the robustness and performance granted by the state feedback control, which could have been lost if we had used only the Kalman filter [36]. For more details about LTR, the reader may refer to [26], [37].

IV. SIMULATIONS AND RESULTS

We implement the proposed control scheme in MAT-LAB/Simulink [38] and run EMT (Electromagnetic Transient) simulations with a time sampling of 10^{-4} s. We design four scenarios with different numbers of DERs in the MG. Then, we validate our results using a MG with high-fidelity DER models to determine if the control scheme we propose achieves parity with respect to optimal individual costs and performance

when compared to a case where the MG has learned DER models. We perform this comparison across all four scenarios.

Second, we compare the cost effectiveness and time-domain performance of three strategies across all four scenarios using high-fidelity DER models: droop control, PI control, and the control scheme we propose.

A. Scenarios description

The four scenarios correspond to 10-kV MGs with different numbers of DERs: (i) 1 PV system and 1 BESS, (ii) 1 PV system and 2 BESS, (iii) 3 PV systems and 3 BESS, (iv) 4 PV systems and 6 BESS. Fig. 1 illustrates scenario 1's MG. The upper-level grid is a 60-Hz stiff grid. All scenarios consider different $q_{i,j}$ and R_i for each DER. For example, in the scenario with 2 DERs, $R_1 = 1, q_{1,1} = 0.5, q_{1,2} = 0.2$ and $R_2 = 1, q_{2,1} = 0.3, q_{2,2} = 0.5$, in this manner, the DERs in competition have different incentives to regulate their power injection as it is explained in Section III-C4. The scenarios simulated consider that the load has the profile shown in the bottom panel of Fig. 4, that the DERs start delivering 10 MW in total, and that the power regulation service starts at t = 0.25 s and ends at t = 6 s. The data we use to generate all the scenarios is publicly available online[1].

B. High-fidelity models and learned models of DERs

We consider a high-order nonlinear PV system model and a BESS model, each has six to eight states, from the Flex-Power Plant model used in [21], [22], [23]. Both high-fidelity DER models include the following Simulink power system devices: a DC-side voltage source, an average VSI model, feed-forward compensation, and a phase-locked loop (PLL). Each DER also includes a current-control loop designed with *dq*-frame PI controllers and feed-forward compensation. The current-control loop receives a power reference input, and then generates PWM signals for VSI to regulate the active power output of the DER.

We learn the dynamics of both high-fidelity DER models using the SI toolbox of MATLAB [38] under a non-linear least squares with automatic line search method. For each DER, the training data consists of input-output timeseries that come from three step responses for six different initial operating points. We validate the learned state-space representation using unseen 18 input-output time-series that come from new step responses. Table I shows the learned state-space representation for each DER type.

As system parameters may vary in practice, we intentionally introduce perturbations (Table II) to the LTR estimator of each DER across all scenarios.

C. Implementation and validation of the control scheme

For each scenario, we compute the Nash strategies (24) using the learned DER models (Table I) and the compensator ($H = 0, G = D = 1$). We implement the resulting controllers in: (a) the MG with learned DER models and (b) the MG with high-fidelity DER models. We underline while (a) simulates

---

[1] https://github.com/REAM-lab/der-control-games

TABLE I
DERs LEARNED STATE-SPACE REPRESENTATIONS

Parameter	PV system	BESS
A	$\begin{bmatrix} -263.094 & -2.955 \cdot 10^4 \\ 1 & 0 \end{bmatrix}$	$\begin{bmatrix} -258.087 & -3.041 \cdot 10^4 \\ 1 & 0 \end{bmatrix}$
B	$\begin{bmatrix} 1 \\ 0 \end{bmatrix}$	$\begin{bmatrix} 1 \\ 0 \end{bmatrix}$
C	$\begin{bmatrix} 1.589 & 2.945 \cdot 10^4 \end{bmatrix}$	$\begin{bmatrix} 9.712 & 3.039 \cdot 10^4 \end{bmatrix}$

TABLE II
PARAMETER PERTURBATIONS INTRODUCED TO THE LTR ESTIMATORS

Parameter	PV system	BESS
ΔA	$\begin{bmatrix} -20 & 1000 \\ 0 & 0 \end{bmatrix}$	$\begin{bmatrix} -100 & 1000 \\ 1 & 0 \end{bmatrix}$
ΔB	$\begin{bmatrix} -0.1 \\ 0 \end{bmatrix}$	$\begin{bmatrix} -0.1 \\ 0 \end{bmatrix}$
ΔC	$\begin{bmatrix} 0.1 & 0.1 \end{bmatrix}$	$\begin{bmatrix} 0.1 & 0.1 \end{bmatrix}$

only the control block diagram in Fig. 2, (b) simulates a three-phase MG with VSIs as we describe in Section IV-B.

We simulate both implementations for each scenario and then, validate if the proposed control scheme in the MG with high-fidelity DER models results in cost solutions and time-domain performance similar to the ones we obtain using learned DER models.

Fig. 3 shows optimal individual costs $J_i(\widetilde{x}_0, \widetilde{w}_0, \widetilde{u}^*)$ for each DER in each scenario for: (a) the MG with learned DER models, and (b) the MG with high-fidelity DER models. For (a), we compute $J_i(\widetilde{x}_0, \widetilde{w}_0, \widetilde{u}^*)$ using the expression in (26), and for (b) we compute it using a trapezoidal integration of (17).

Fig. 3 reveals that $J_i(\widetilde{x}_0, \widetilde{w}_0, \widetilde{u}^*)$ for any DER i in (b) is slightly greater than its corresponding value in (a). In fact, as more DERs are integrated into the MG, this difference increases, although only marginally from 1.98% up to 6.63%. This confirms that (b) reaches parity in optimal individual costs with (a).

The top panel of Fig. 4 shows the MG's power output trajectory in (a) and (b). Both correspond to a MG with ten DERs using our proposed control scheme. We observe that (i) the MG's power output tracks the power reference despite transient deviations caused by load perturbations, and (ii) the trajectory of (a) is very close to the trajectory of (b) throughout the power regulation service.

To illustrate the two previous observations, the top panel of Fig. 4 shows the real-time response in more detail. We also notice that despite the MG's power output deviating from the power reference due to load perturbations, the proposed control scheme is able to steer it back to the reference. For instance, we see that the (a) and (b) increases from the -14-MW requested power up to -9 MW and -9.36 MW, respectively, at t = 4.5 s because of the sudden 8-MW load decline. Then, (a) and (b) come back to -14MW±5% at t = 4.64 s and t = 4.65 s, respectively.
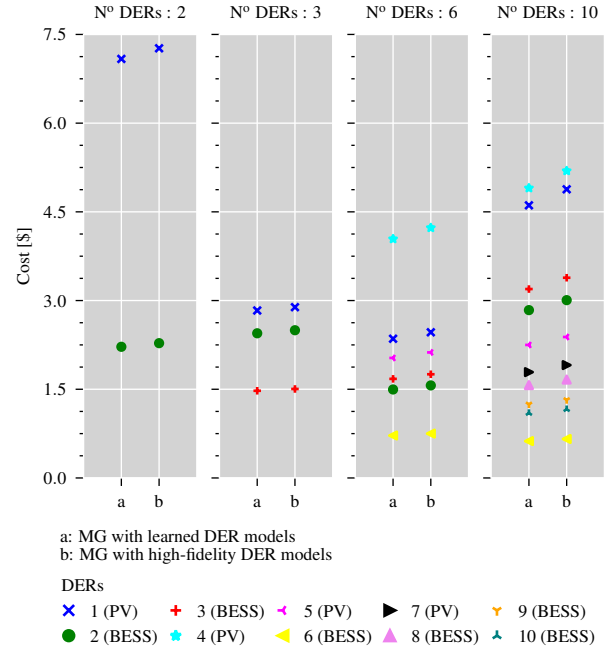

Fig. 3. Optimal individual costs for each DER in case: (a) the microgrid (MG) with learned DER models and (b) the MG with high-fidelity DER models for all four scenarios.

Table III shows the maximum of each performance parameter over the simulation time for (a) and (b) for the four scenarios. We note that the error columns range between -6.7% and 0.3%. Hence, the analysis of Fig. 4 and Table III confirms that (b) reaches almost parity in time-domain performance with (a).
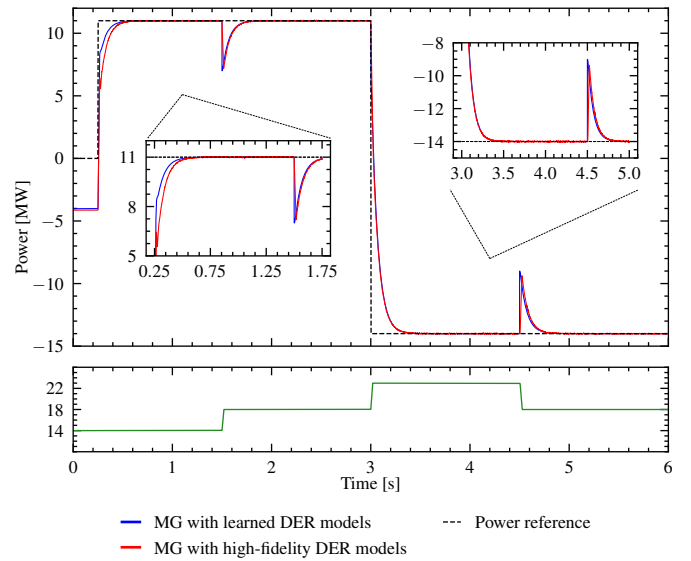

Fig. 4. Top panel: Microgrid (MG)'s power output with learned DER models and MG's power output with high-fidelity DER models. The MG's power output is the power delivered to the upper-level grid that must track a power reference. Bottom panel: MG's load during the regulation service.

TABLE III
MG'S PERFORMANCE USING THE CONTROL SCHEME WE PROPOSE

DERs	Overshoot (%)			Settling time (s)			Steady-state error (%)		
	a	b	error (%)	a	b	error (%)	a	b	error (%)
2	-36.4	-35.7	-1.9	0.42	0.42	0	0	0	0
3	-36.4	-35.1	-3.5	0.26	0.26	0	0	0	0
6	-36.4	-33.9	-6.7	0.21	0.21	0	0	0.2	0.2
10	-36.4	-34.6	-4.8	0.23	0.23	0	0	0.3	0.3

a: Microgrid's power output with learned DER models
b: Microgrid's power output with high-fidelity DER models

D. Comparison between droop control, PI control, and the control scheme we propose

We tune the droop and PI controllers for each scenario as follows: 1) We run the simulation with the control scheme we propose, 2) we calculate a power share for each DER that results from the division of its power injection in steady-state by the total DERs' power output, 3) we set the gains of the droop and PI to the power shares, 4) we slightly tweak the gains to reduce the steady-state error, and to try to have an overshoot less than 30% and a settling time less than 0.65 s. The latter step is the most demanding, particularly when the number of DERs increases, because more gains are simultaneously tuned with back-to-back simulations.

Table IV shows, most notably, that the proposed control scheme for a MG with one DER results in saving between 28.3 up to 209 times relative to using droop control, and between 1.3 up to 9.3 times relative to using PI control. We also note that some DERs can obtain greater savings than others under the proposed control scheme.

TABLE IV
SAVINGS USING THE CONTROL SCHEME WE PROPOSE FOR ALL 4 SCENARIOS

Savings relative to:	DERs									
	1	2	3	4	5	6	7	8	9	10
Droop	28.3	34.2								
PI	1.3	1.5								
Droop	100	116	123							
PI	3.6	4.1	4.3							
Droop	209	185	204	189	196	171				
PI	9.3	8.3	9.1	8.5	8.8	7.7				
Droop	48.5	50.9	54.2	53.3	51.2	37.0	50.5	51.3	48.7	46.8
PI	7.3	7.6	8.1	8.0	7.7	5.7	7.6	7.7	7.3	7.1

The saving relative to droop control is $J_i(\widetilde{x}_0, \widetilde{w}_0, \widetilde{u}^*)/J_i(\widetilde{x}_0, \widetilde{w}_0, \widetilde{u}^{\text{droop}})$
The saving relative to PI control is $J_i(\widetilde{x}_0, \widetilde{w}_0, \widetilde{u}^*)/J_i(\widetilde{x}_0, \widetilde{w}_0, \widetilde{u}^{\text{PI}})$

Fig. 5 shows the time-domain trajectories of the MG's power output for the three control schemes at each scenario, and Table V reports their maximum performance parameters over the time simulation. The damping shown in Table V is the damping of the dominant poles of the third-order transfer function that estimates the MG's power output response.

In Fig. 5, the droop and PI control result in a high number of oscillations in the transient which translates in low damping

ratios ranging from 0.06 up to 0.53 as Table V shows. In contrast, the proposed control scheme results in having no oscillations, i.e., a damping ratio equal to 1. Despite this over-damped trajectory, Table V shows that the proposed control scheme results in 1.64 up to 3 times faster settling times than the PI control across all the scenarios.

Table V also indicates that, despite achieving faster settling times compared to the proposed control scheme, the droop controller is always outperformed with respect to the steady-state error. In particular, the steady-state error the droop controller achieves is, at its best, 15.7%. In Fig. 5, we also observe that although the proposed control scheme does not produce any overshoot when power regulation begins at t = 0.25 s and the requested power changes at t = 3 s, it leads to greater decays (negative overshoot) compared to the PI and droop control in all scenarios whenever there is a sudden load increase and decrease at times t = 1.5 s and t = 4.5 s, respectively.

Therefore, the control scheme we propose outperforms the standard controllers (droop and PI), since it results in lower individual costs for the DERs and a better time-domain performance across the different metrics.

TABLE V
MG'S PERFORMANCE FOR THREE CONTROL SCHEMES IN ALL FOUR SCENARIOS

DERs	Control	Overshoot (%)	Settling time (s)	steady-state error (%)	Damping (ζ)
2	Droop	-65.5	0.09	37.67	0.12
	PI	-56.02	0.69	1.2	0.12
	Proposed	-35.67	0.42	0.01	1
3	Droop	-61.36	0.1	28.88	0.25
	PI	-17.74	0.61	0.24	0.13
	Proposed	-35.09	0.26	0	1
6	Droop	-37.37	0.07	28.96	0.06
	PI	21.61	0.63	0.69	0.10
	Proposed	-33.93	0.21	0	1
10	Droop	-54	0.19	15.7	0.53
	PI	22.15	0.68	0.66	0.09
	Proposed	-34.6	0.23	0.02	1

V. RECOMMENDATIONS FOR SYSTEM OPERATORS

A practical application of the proposed control scheme is the control of a DER-populated neighborhood for the provision of *fast ancillary services*. In this setting, the PV systems and BESS of the households can be coordinated by the proposed control scheme to provide power injections for a horizon of 2 - 5 seconds at the operator's request. In this manner, the DER-populated neighborhood can improve the frequency nadir of the transmission network.

The control scheme we propose requires communication channels between the DERs to inform the full DERs' estimated states in real time. Hence, DERs' owners should commit to sharing the full state of their DERs during the provision of the regulation service, otherwise the control scheme may not
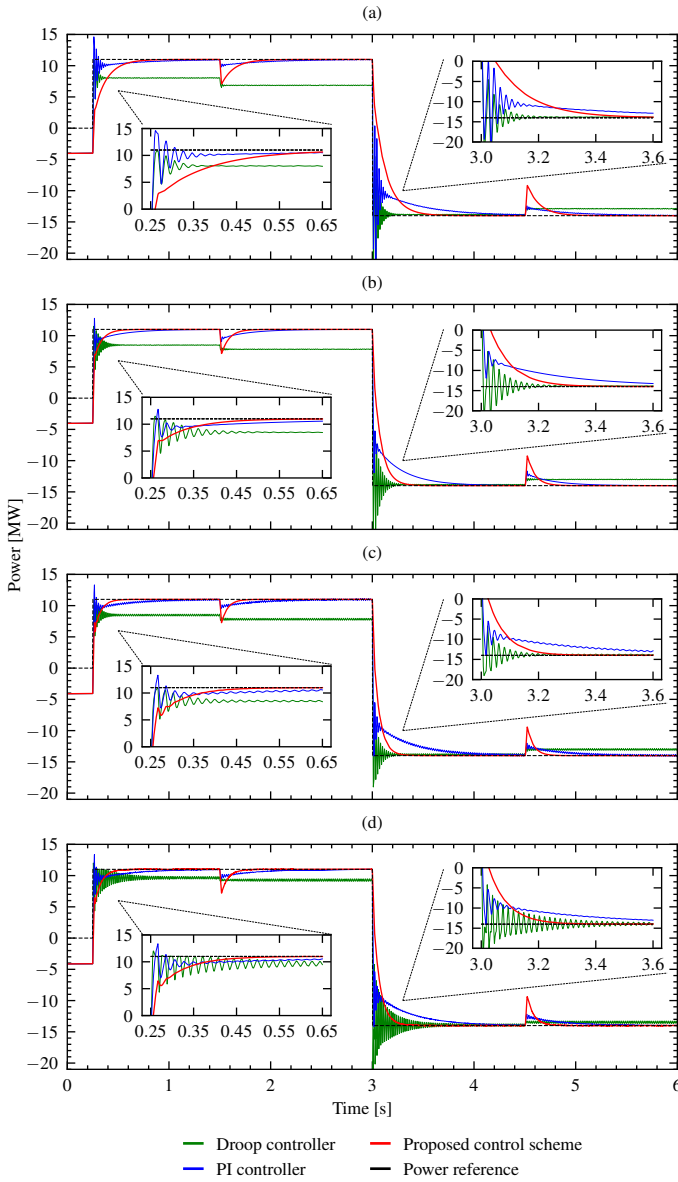
Fig. 5. Microgrid's power delivered to the upper grid under three control schemes (Droop control, PI control, and proposed control scheme) for: (a) scenario 1 (two DERs), (b) scenario 2 (three DERs), (c) scenario 3 (six DERs), and (d) scenario 4 (ten DERs).

the matrices $(\bar{A}, \begin{bmatrix} \bar{B}_1 & ... & \bar{B}_N \end{bmatrix})$ to be stabilizable which is a necessary and sufficient condition for the existence of a Nash equilibrium solution for the control scheme. In the worst case, when some DERs suddenly abandon the regulation service, the feedback controller from the other DERs may still bring the tracking error to zero, which implies that the MG may still be able to comply with the power regulation. This is because the nature of the controller we propose is an integral-action type as we see using (9) and (22): $u_i^* = K_i x + F_i w = K_i x + F_i \int (r - Cx(t)) dt$. However, there could be capacity constraints when some DERs suddenly leave the regulation service. The power injection of the remaining DERs will increase to try to comply with the regulation service, and this event may cause overloading on the DERs. In addition, the controllers may not be able to ensure a Nash equilibrium solution anymore. In practice, to avoid these consequences, the operator should inform that the DERs that desire to participate in the regulation service should not desert in the middle of the regulation service, otherwise they would be financially penalized.

VI. Conclusions

We have introduced a novel control scheme capable of reducing individual costs for DERs and improving the time-domain performance of the MG when compared to classical control techniques like droop control and PI control. Two virtues of the proposed control scheme are that: (i) it employs learned VSI dynamics that reduce the complexity of deriving and computing the full dynamical model of DERs with *dq*-control schemes, and (ii) that it considers the potentially selfish nature of DERs using non-cooperative game theory and realistic DER dynamics.

The control scheme we design works in time intervals of seconds. For longer periods of control, e.g., minutes or hours, future work may focus on including energy constraints such as the state of charge of BESS, time-varying irradiance for the PV panels, and installed power rating constraints. Another future direction may be the design of a differential-game-theory-based control scheme in which the frequency is a state and the dynamics of the VSC are incorporated; in this manner, generators and VSCs will compete to restore the frequency deviation back to zero.

work since it is not designed to work with partial information of the DERs' states. In addition, the communication channels required by the control scheme may be an open door for cyber-attacks and communication delays that could degrade the performance of the control scheme. We identify as an interesting and impactful future direction to explore how to reformulate the controller scheme to only rely on partial information of the systems' states while still performing well and providing safety certificates.

Finally, although the proposed control scheme considers DERs as selfish agents that minimize their individual costs, it requires all DERs to commit so the MG can comply with the power regulation service. This latter consideration secures

References

[1] D. E. Ochoa, F. Galarza-Jimenez, F. Wilches-Bernal, D. A. Schoenwald, and J. I. Poveda, "Control systems for low-inertia power grids: A survey on virtual power plants," *IEEE Access*, vol. 11, pp. 20 560–20 581, 2023.

[2] M. H. Saeed, W. Fangzong, B. A. Kalwar, and S. Iqbal, "A review on microgrids' challenges & perspectives," *IEEE Access*, vol. 9, pp. 166 502–166 517, 2021.

[3] N. Naval and J. M. Yusta, "Virtual power plant models and electricity markets - a review," *Renewable and Sustainable Energy Reviews*, vol. 149, p. 111393, 2021. [Online]. Available: https://www.sciencedirect.com/science/article/pii/S136403212100678X

[4] K. Bala Ganesh, R. Vijay, and P. Mathuria, "Ancillary services from ders for transmission and distribution system operators," in *2022 22nd National Power Systems Conference (NPSC)*, 2022, pp. 482–487.

[5] S. Skok, R. Gulam, M. Balkovic, and K. Ugarkovic, "Analysis of ancillary services provided by distributed energy resources in smart distribution grid," in *2022 3rd International Conference on Intelligent Engineering and Management (ICIEM)*, 2022, pp. 68–74.

[6] B. Marinescu, O. Gomis-Bellmunt, F. Dörfler, H. Schulte, and L. Sigrist, "Dynamic virtual power plant: A new concept for grid integration of renewable energy sources," *IEEE Access*, vol. 10, pp. 104 980–104 995, 2022.

[7] F. Gulotta, E. Daccò, A. Bosisio, and D. Falabretti, "Opening of ancillary service markets to distributed energy resources: A review," *Energies*, vol. 16, no. 6, 2023. [Online]. Available: https://www.mdpi.com/1996-1073/16/6/2814

[8] E. Dall'Anese, S. S. Guggilam, A. Simonetto, Y. C. Chen, and S. V. Dhople, "Optimal regulation of virtual power plants," *IEEE Transactions on Power Systems*, vol. 33, no. 2, pp. 1868–1881, 2018.

[9] B. Behi, P. Jennings, A. Arefi, A. Azizivahed, A. Pivrikas, S. M. Muyeen, and A. Gorjy, "A robust participation in the load following ancillary service and energy markets for a virtual power plant in western australia," *Energies*, vol. 16, no. 7, 2023. [Online]. Available: https://www.mdpi.com/1996-1073/16/7/3054

[10] C. P. Guzman, N. Bañol Arias, J. F. Franco, M. J. Rider, and R. Romero, "Enhanced coordination strategy for an aggregator of distributed energy resources participating in the day-ahead reserve market," *Energies*, vol. 13, no. 8, 2020. [Online]. Available: https://www.mdpi.com/1996-1073/13/8/1965

[11] Y. Zhu, T. Mao, G. Zhan, Q. Ai, and S. Yin, "Optimal scheduling model for virtual power plant participating in energy and regulation markets," in *2022 7th Asia Conference on Power and Electrical Engineering (ACPEE)*, 2022, pp. 447–453.

[12] Y. Chen, Z. Li, S. S. Yu, B. Liu, and X. Chen, "A profitability optimization approach of virtual power plants comprised of residential and industrial microgrids for demand-side ancillary services," *Sustainable Energy, Grids and Networks*, vol. 38, p. 101289, 2024. [Online]. Available: https://www.sciencedirect.com/science/article/pii/S2352467724000183

[13] L. Wang, J. Kwon, N. Schulz, and Z. Zhou, "Evaluation of aggregated ev flexibility with tso-dso coordination," *IEEE Transactions on Sustainable Energy*, vol. 13, no. 4, pp. 2304–2315, 2022.

[14] L. Cheng and T. Yu, "Game-theoretic approaches applied to transactions in the open and ever-growing electricity markets from the perspective of power demand response: An overview," *IEEE Access*, vol. 7, pp. 25 727–25 762, 2019.

[15] X. Chen and K.-C. Leung, "Non-cooperative and cooperative optimization of scheduling with vehicle-to-grid regulation services," *IEEE Transactions on Vehicular Technology*, vol. 69, no. 1, pp. 114–130, 2020.

[16] J. Tan and L. Wang, "Coordinated optimization of phevs for frequency regulation capacity bids using hierarchical game," in *2015 IEEE Power & Energy Society General Meeting*, 2015, pp. 1–5.

[17] X. Sun, H. Xie, D. Qiu, Y. Xiao, Z. Bie, and G. Strbac, "Decentralized frequency regulation service provision for virtual power plants: A best response potential game approach," *Applied Energy*, vol. 352, p. 121987, 2023. [Online]. Available: https://www.sciencedirect.com/science/article/pii/S030626192301351X

[18] X. Li, C. Li, F. Luo, G. Chen, Z. Y. Dong, and T. Huang, "Electric vehicles charging dispatch and optimal bidding for frequency regulation based on intuitionistic fuzzy decision making," *IEEE Transactions on Fuzzy Systems*, vol. 31, no. 2, pp. 596–608, 2023.

[19] J. Zhang, Y. Gao, P. Yu, B. Li, Y. Yang, Y. Shi, and L. Zhao, "Coordination control of multiple micro sources in islanded microgrid based on differential games theory," *International Journal of Electrical Power & Energy Systems*, vol. 97, pp. 11–16, 2018.

[20] T. Mylvaganam and A. Astolfi, "Control of microgrids using a differential game theoretic framework," in *2015 54th IEEE Conference on Decision and Control (CDC)*, 2015, pp. 5839–5844.

[21] T. Haines, F. Wilches-Bernal, R. Darbali-Zamora, and M. Jiménez-Aparicio, "Flexible control of synthetic inertia in co-located clusters of inverter-based resources," in *2022 IEEE Power and Energy Conference at Illinois (PECI)*, 2022, pp. 1–6.

[22] F. Wilches-Bernal, T. Haines, R. Darbali-Zamora, and M. Jiménez-Aparicio, "A resource aware droop control strategy for a pv, wind, and energy storage flexible power (flexpower) plant," in *2022 IEEE Kansas Power and Energy Conference (KPEC)*, 2022, pp. 1–5.

[23] T. Haines, R. Darbali-Zamora, M. Jiménez-Aparicio, and F. Wilches-Bernal, "The impact of co-located clusters of inverter-based resources on a performance-based regulation market metric," in *2022 North American Power Symposium (NAPS)*, 2022, pp. 1–6.

[24] A. Yazdani and R. Iravani, *Voltage-Sourced Converters in Power Systems*. John Wiley & Sons, Ltd, 2010.

[25] L. Ljung, "Perspectives on system identification," *IFAC Proceedings Volumes*, vol. 41, no. 2, pp. 7172–7184, 2008, 17th IFAC World Congress. [Online]. Available: https://www.sciencedirect.com/science/article/pii/S1474667016400984

[26] F. L. Lewis, D. Vrabie, and V. L. Syrmos, *Optimal Control*. John Wiley & Sons, Ltd, 2012. [Online]. Available: https://onlinelibrary.wiley.com/doi/abs/10.1002/9781118122631.fmatter

[27] D. Cappello and T. Mylvaganam, "Approximate Nash equilibrium solutions of linear quadratic differential games," *IFAC-PapersOnLine*, vol. 53, no. 2, pp. 6685–6690, 2020, 21st IFAC World Congress. [Online]. Available: https://www.sciencedirect.com/science/article/pii/S2405896320303475

[28] J. C. Engwerda and Salmah, "Necessary and sufficient conditions for feedback Nash equilibria for the affine-quadratic differential game," *Journal of Optimization Theory and Applications*, vol. 157, no. 2, pp. 552–563, May 2013. [Online]. Available: https://doi.org/10.1007/s10957-012-0188-1

[29] J. F. Nash Jr, "Equilibrium points in n-person games," *Proceedings of the national academy of sciences*, vol. 36, no. 1, pp. 48–49, 1950.

[30] J. Engwerda, *LQ dynamic optimization and differential games*. Chicester, West Sussex, England ;: J. Wiley & Sons, 2005.

[31] C. Gallegos, "Solving the coupled riccati equation for the n-players lq differential game," in *2005 2nd International Conference on Electrical and Electronics Engineering*, 2005, pp. 365–369.

[32] J. Engwerda, "A numerical algorithm to calculate the unique feedback Nash equilibrium in a large scalar lq differential game," *Dynamic Games and Applications*, vol. 7, no. 4, pp. 635–656, Dec 2017. [Online]. Available: https://doi.org/10.1007/s13235-016-0201-7

[33] T. Damm, V. Dragan, and G. Freiling, "Coupled riccati differential equations arising in connection with Nash differential games," *IFAC Proceedings Volumes*, vol. 41, no. 2, pp. 3946–3951, 2008, 17th IFAC World Congress. [Online]. Available: https://www.sciencedirect.com/science/article/pii/S1474667016395623

[34] L. Jódar, "Solving coupled riccati matrix differential systems," *Applied Mathematics Letters*, vol. 4, no. 1, pp. 17–19, 1991. [Online]. Available: https://www.sciencedirect.com/science/article/pii/089396599190114B

[35] J. Engwerda, "Algorithms for computing nash equilibria in deterministic lq games," *Computational Management Science*, vol. 4, no. 2, pp. 113–140, Apr 2007. [Online]. Available: https://doi.org/10.1007/s10287-006-0030-z

[36] J. Doyle, "Guaranteed margins for lqg regulators," *IEEE Transactions on Automatic Control*, vol. 23, no. 4, pp. 756–757, 1978.

[37] G. Stein and M. Athans, "The lqg/ltr procedure for multivariable feedback control design," *IEEE Transactions on Automatic Control*, vol. 32, no. 2, pp. 105–114, 1987.

[38] The MathWorks Inc., "Matlab version: 9.14.0 (r2023a)," Natick, Massachusetts, United States, 2023. [Online]. Available: https://www.mathworks.com